Nuclear-quadrupole-resonance study of overdoped $Y_{1-x}Ca_xBa_2Cu_3O_7$

G. V. M. Williams,[1,2] S. Krämer,[2] and M. Mehring[2]
[1]The New Zealand Institute for Industrial Research, P.O. Box 31310, Lower Hutt, New Zealand
[2]Physikalisches Institut, Universität Stuttgart, D-70550 Stuttgart, Germany
(Received 20 March 2000; published 20 February 2001)

We have performed a ^{63,65}Cu nuclear-quadrupole-resonance study of overdoped $Y_{1-x}Ca_xBa_2Cu_3O_7$ and find that the temperature dependence of the Cu spin-lattice and spin-spin relaxation rates are similar to that in lightly overdoped $YBa_2Cu_3O_7$. We show that the data can be interpreted within the Millis, Monien, and Pines model in terms of no significant decrease in the antiferromagnetic correlation length, at least for $p<0.233$. Furthermore, the isotopic ratios of the spin-lattice and spin-spin relaxation rates do not change with increasing hole concentration, indicating that magnetic relaxation is still dominant in the overdoped region.

DOI: 10.1103/PhysRevB.63.104514 PACS number(s): 74.72.Bk, 74.25.Nf, 74.20.Mn

The high-temperature superconducting cuprates (HTSC) are proving to be extremely difficult to understand. The difficulty in understanding these materials is compounded by recent reports that suggest that antiferromagnetic correlations do not exist in overdoped ($p>0.16$) $YBa_2Cu_3O_{7-\delta}$ and $Bi_2Sr_2CaCu_2O_{8+\delta}$, possibly disappearing for hole concentrations $p>0.19$.[1,2] Indeed, there is evidence from low-temperature low-energy neutron-scattering measurements on $La_{2-x}Sr_xCuO_4$ that the low-temperature antiferromagnetic correlation length is weakly hole concentration dependent for underdoped to lightly overdoped $La_{2-x}Sr_xCuO_4$ ($p<0.18$) and decreases substantially in the heavily overdoped region ($p\sim0.25$).[3]

The possible absence of antiferromagnetic correlations for overdoped HTSC has important implications for understanding superconductivity and interpreting the nuclear-magnetic-resonance (NMR) data from the HTSC. It is currently believed that the NMR data can be interpreted within the Millis, Monien, and Pines (MMP) model.[4–7] MMP proposed a phenomenological dynamical spin susceptibility that, along with the Mila-Rice Hamiltonian,[5] has been used to interpret the NMR data. In this model the dynamical spin susceptibility is peaked at the antiferromagnetic wave vector, which strongly enhances the Cu spin-lattice relaxation rate but not the ^{17}O spin-lattice relaxation rate. The MMP model is also the basis of the nearly antiferromagnetic Fermi-liquid (NAFL) model[8–10] of HTSC. This single-spin fluid model assumes the presence of antiferromagnetic correlations across the entire superconducting phase diagram, *including the overdoped side*. Thus, if antiferromagnetic correlations do not exist on the overdoped side then the MMP phenomenological susceptibility cannot be used to interpret the NMR data and the NAFL model cannot be applied to overdoped HTSC. It is therefore important to extend previous studies into the overdoped region.

In this paper, we report Cu nuclear-quadrupole-resonance (NQR) measurements on overdoped $Y_{1-x}Ca_xBa_2Cu_3O_7$ and compare the results with optimally doped and lightly overdoped $YBa_2Cu_3O_{7-\delta}$. The addition of Ca allows us to extend previous $YBa_2Cu_3O_{7-\delta}$ studies[11–14] into the heavily overdoped region. We selected the $Y_{1-x}Ca_xBa_2Cu_3O_7$ compound rather than $La_{2-x}Sr_xCuO_4$ because the $La_{2-x}Sr_xCuO_4$ NQR linewidths are anomalously large (~2 MHz). Furthermore, there is evidence from the NQR spectra of two Cu sites in the CuO_2 plane as well as a Cu spin-lattice relaxation rate that is frequency dependent.[15] We compare the spin-lattice and spin-spin relaxation rates in the overdoped region with similar measurements in the underdoped to lightly overdoped region.[11–14]

Overdoped $Y_{1-x}Ca_xBa_2Cu_3O_{7-\delta}$ ceramic samples were synthesized as described previously.[16] The final synthesis at 980 °C in 1 bar O_2 was followed by rapid cooling to 600 °C and further annealing to 350 °C to ensure that the samples were fully oxygen loaded.

The superconducting transition temperature was measured using a superconducting quantum interference device magnetometer and an applied magnetic field of 0.0005 T. Room-temperature thermopower measurements were made using a technique described previously.[17]

Cu NQR measurements were made in a home-built probe as previously described.[14] The influence of external fields was minimized by surrounding the probe and continuous flow cryostat with a μ-metal shield. The spin-lattice relaxation rate was measured using an inversion recovery pulse sequence and a $\pi/2$ pulse width of 2 μs. The spin-spin relaxation rate was measured using a Hahn-echo pulse sequence with the same pulse widths. Doubling the $\pi/2$ pulse width did not lead to a significant variation in the spin-spin relaxation rate. This is consistent with a previous study on $YBa_2Cu_3O_{7-\delta}$, where $1/T_{2g}$ was not found to change when H_1 was varied by a factor of 2.[14]

The magnetization recovery in the case of the Cu NQR spin-lattice relaxation measurements can be expressed as $M(\tau)=M_0[1-2\exp(-3\tau/T_1)]$, where $1/T_1$ is the spin-lattice relaxation rate. The Cu NQR spin-echo decay in the case of the T_2 measurement is more complicated. It has been shown that the echo decay function can be expressed as[18,19]

$$M(\tau)=M_0\exp\left(-\frac{2\tau}{T_{2R}}\right)\exp\left(-\frac{1}{2}\frac{(2\tau)^2}{T_{2g}^2}\right)M_d(2\tau). \quad (1)$$

The first factor is the Redfield contribution, where for $YBa_2Cu_3O_7$ $T_{2R}^{-1}=5.1T_1^{-1}$.[20] The second factor is the Gaussian decay function. The third factor has recently been introduced to account for the dynamical effects of the nearest-neighbor Cu sites. This factor is close to 1 when

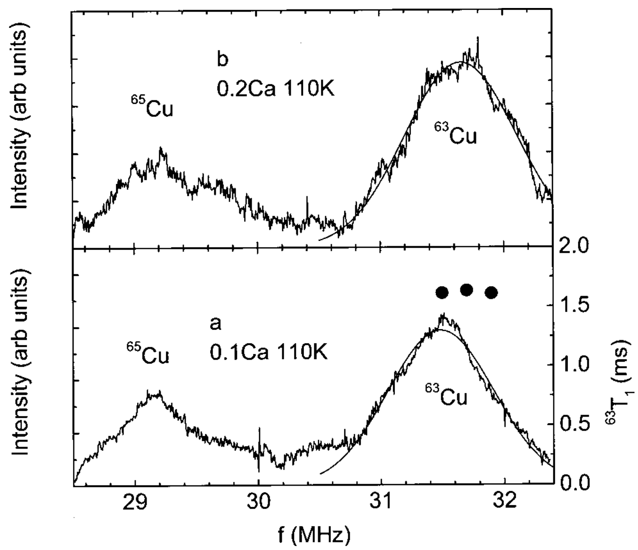

FIG. 1. (a) Plot of the Cu NQR spectra at 110 K from fully loaded $Y_{0.9}Ca_{0.1}Ba_2Cu_3O_7$ (left axis). Also plotted is the frequency dependence of $^{63}T_1$ (right axis). (b) Plot of the Cu NQR spectra at 110 K from $Y_{0.8}Ca_{0.2}Ba_2Cu_3O_7$. The solid curve is a Gaussian best fit to the ^{63}Cu NQR resonance.

$T_{1,\mathrm{NQR}} \gg T_{2g}$. The functional form for $M_d(\tau)$ can be found in recent publications by Curro *et al.*[18,19]

We present in Fig. 1 the Cu NQR spectra from the $x=0.1$ [Fig. 1(a)] and $x=0.2$ [Fig. 1(b)] samples at 110 K. The spectra were obtained by summing the spectra measured at discrete frequencies. The superconducting transition temperatures for the $x=0.1$ and 0.2 samples are 68 and 48 K, respectively. We estimate the hole concentrations p from the approximate relation $T_c/T_{c,\mathrm{Max}}=1-82.6(p-0.16)^2$ (Ref. 21) to be 0.214 and 0.233, respectively. The negative room-temperature thermopower values are consistent with the samples being overdoped ($p>0.16$).

The main peaks observed in the NQR spectra plotted in Fig. 1 are due to Cu from the CuO_2 planes, where the relative integrated intensities of the ^{65}Cu and ^{63}Cu peaks are directly proportional to the isotopic abundance. We did not find any variation in the NQR linewidths with temperature for temperatures greater than 60 K.

We estimate the ^{63}Cu full-width half maximum (FWHM) for Cu on the CuO_2 planes by fitting the resonance of the ^{63}Cu peak to a Gaussian function. The resultant FWHM's are 850 kHz for $x=0.1$ and 900 kHz for $x=0.2$. The ^{63}Cu NQR linewidths can be compared with fully loaded $YBa_2Cu_3O_{7-\delta}$, where the smallest reported NQR linewidth is ~250 kHz.[22] Most of the additional broadening is likely to be due to oxygen vacancies in the CuO chains. It has been found that the Cu NQR linewidth increases dramatically with increasing oxygen vacancies on the CuO chain.[23] Evidence of oxygen vacancies is provided by the additional intensity in between the ^{63}Cu and ^{65}Cu NQR peaks. It is also possible that some of the additional broadening is due to local site disorder about the Ca atom. This has been suggested to explain the nearly threefold increase in the ^{63}Cu NQR linewidth from Cu in the CuO_2 planes of $Y_{0.9}Ca_{0.1}Ba_2Cu_4O_8$ when compared with $YBa_2Cu_4O_8$.[24] We note that the NQR peak frequency for both the $x=0.1$ and 0.2 samples is comparable to that found in optimally doped $YBa_2Cu_3O_{7-\delta}$.[25] We also find that the ^{63}Cu NQR peak frequency is larger for the $x=0.2$ Ca, which is consistent with the $x=0.2$ Ca sample having a higher hole concentration.

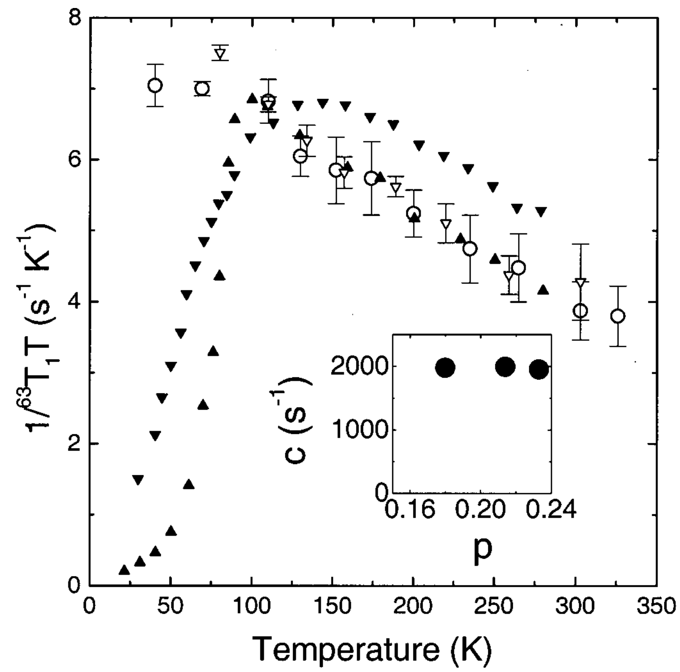

FIG. 2. Plot of $1/^{63}T_1T$ against temperature from $YBa_2Cu_3O_{6.63}$ [filled down triangles (Ref. 11)], $YBa_2Cu_3O_7$ [filled up triangles (Ref. 27)], $Y_{0.9}Ca_{0.1}Ba_2Cu_3O_7$ (open down triangles), and $Y_{0.8}Ca_{0.2}Ba_2Cu_3O_7$ (open circles). Plot of the Curie constant against hole concentration obtained by fitting the data in the figure for $T>100$ K as described in the text.

We find that although our spectra are broad, the Cu T_1 magnetization recovery is single exponential. The Cu NQR recovery is expected to be single exponential in an homogeneous material because Cu is a spin $\frac{3}{2}$ nuclei and thus the nuclear-quadrupole interaction leads to only one transition. The exponential magnetization recovery in $Y_{1-x}Ca_xBa_2Cu_3O_7$ can be contrasted with $YBa_2(Cu_{1-y}Zn_y)_3O_{7-\delta}$ (Ref. 26), where Zn induces a nonexponential magnetization recovery. We show in Fig. 1(a) (filled circles) that $^{63}T_1$ is not frequency dependent.

It can be seen in Fig. 2 that the temperature dependence of $1/^{63}T_1T$ for overdoped $x=0.1$ (open down triangles, $p=0.214$) and $x=0.2$ (open circles, $p=0.233$) is comparable to that of fully loaded $YBa_2Cu_3O_7$ as measured by Hammel *et al.* (solid up triangles, $p=0.18$).[27] There is no evidence of a change in the Curie-like behavior for temperatures greater than 100 K. This is clear in the inset to Fig. 2, where we plot the Curie constant c, obtained by fitting the data above 100 K to $1/^{63}T_1T=c/(T+T_0)+b$, where the best fit is obtained with $T_0=180$ K. In the case of underdoped $YBa_2Cu_3O_{7-\delta}$ (solid down triangles[12]) there is the added complication of the normal-state pseudogap that causes $1/^{63}T_1T$ to decrease for temperatures less than 140 K.[28]

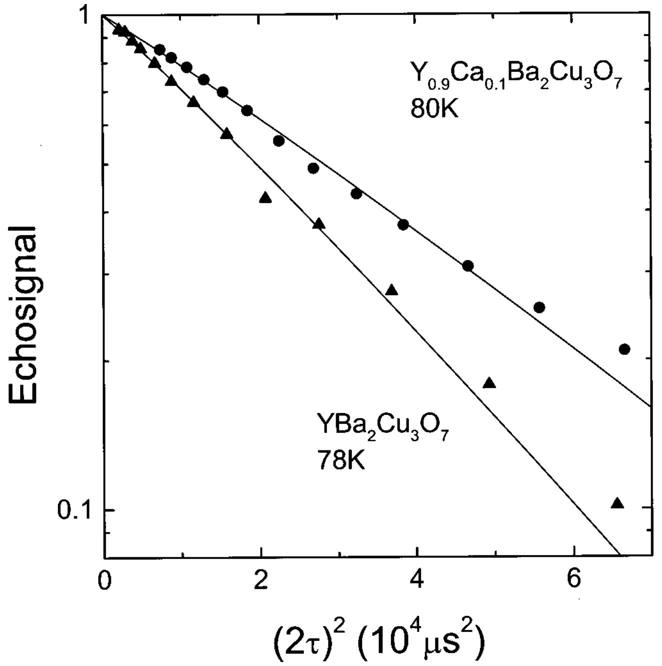

FIG. 3. Plot of the normalized ^{63}Cu NQR spin-echo magnetization against $(2\tau)^2$ from $Y_{0.9}Ca_{0.1}Ba_2Cu_3O_7$ (filled circles) at 80 K and from $YBa_2Cu_3O_7$ (filled up triangles) at 78 K (Ref. 14). The solid curve is a fit to the data as described in the text.

The common $1/^{63}T_1T$ curve for the overdoped $x=0$, 0.1, and 0.2 samples suggests that there is no significant change in the spin dynamics as probed by ^{63}Cu. It is also possible to interpret the overdoped $1/^{63}T_1T$ data plotted in Fig. 2, within the MMP model and the scaling analysis of Barzykin and Pines (BP),[6] in terms of no significant change in the antiferromagnetic correlation length. This can be understood by noting that the Curie-like increase in $1/^{63}T_1T$ with decreasing temperature is generally believed to be due to changes in the imaginary part of the dynamical spin susceptibility.[6,10,18] It is also generally believed that the NMR data can be analyzed using the MMP dynamical spin susceptibility,[4] which can be expressed as

$$\chi(\mathbf{q},\omega)=\frac{\beta\xi^2}{1+(\mathbf{Q}-\mathbf{q})^2\xi^2-i\omega/\omega_{sf}}+\frac{\chi_s(T)}{1-i\omega/\Gamma_0}, \quad (2)$$

where ω_{sf} is the paramagnon frequency, ξ is the antiferromagnetic correlation length in units of the in-plane lattice parameter, $\mathbf{Q}=(\pi,\pi)$ is the antiferromagnetic wave vector, $\chi_s(T)$ is the static spin susceptibility, and Γ_0 is the temperature-independent effective bandwidth. It has been shown that in the limit of $\xi\gg 1$, $(^{63}T_1T)^{-1}=a_1\beta/\omega_{sf}$.[6] In the scaling-analysis model of BP, $\omega_{sf}\propto\xi^{-z}$, where $z=1$ for $T^*\leqslant T\leqslant T_{cr}$ and $z=2$ for $T>T_{cr}$. Consequently, $(^{63}T_1T)^{-1}\propto\beta\xi^z$. The scaling of $(^{63}T_1T)^{-1}$ and $^{63}T_{2g}^{-2}$ for slightly overdoped $YBa_2Cu_3O_{7-\delta}$ implies that $z=1$ for $T>100$ K and hence $(^{63}T_1T)^{-1}\propto\beta\xi$.[29] Therefore, within the MMP model and using the scaling analysis of BP, we expect that $(^{63}T_1T)^{-1}$ is directly proportional to ξ for overdoped $Y_{1-x}Ca_xBa_2Cu_3O_7$ and thus the constant $(^{63}T_1T)^{-1}$ for $x=0$, 0.1, and 0.2 above 100 K implies that there is no change in ξ for $0.18\leqslant p\leqslant 0.233$. We note that within the MMP model β is assumed to be temperature independent. However, we have shown that equating β with the static spin susceptibility $\chi(T)$ can explain the ^{17}O and ^{63}Cu NMR data in underdoped $YBa_2Cu_4O_8$, where $\chi(T)$ rapidly decreases with increasing temperature.[2,30,31] In the case of overdoped $Y_{1-x}Ca_xBa_2Cu_3O_7$, the maximum increase in $\chi(T)$ is only 14% from 300 to 100 K (Ref. 16) and hence any temperature variation in β is not expected to significantly affect the interpretation of our data.

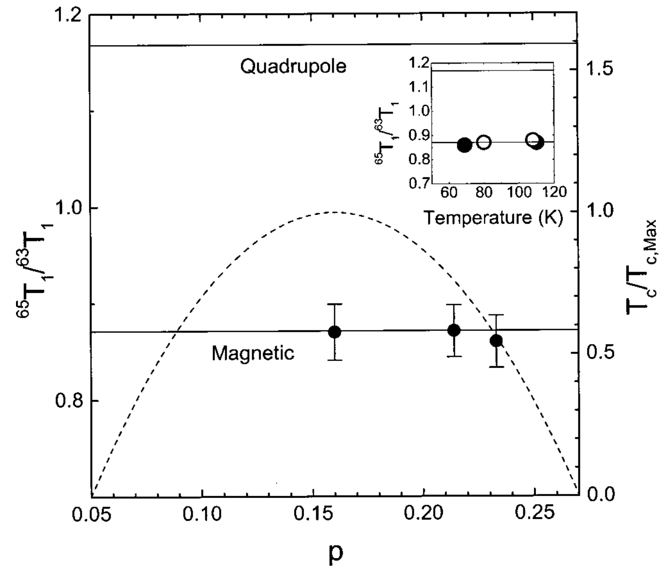

FIG. 4. Plot of the measured ratio $^{65}T_1/^{63}T_1$ against hole concentration (filled circles and left axis). The $YBa_2Cu_3O_{7-\delta}$ data (Ref. 32) was obtained near 60 K and the $Y_{0.9}Ca_{0.1}Ba_2Cu_3O_7$ and $Y_{0.8}Ca_{0.2}Ba_2Cu_3O_7$ data was obtained at 80 and 68 K, respectively. The dashed line (right axis) is the universal curve that describes the dependence of T_c on hole concentration. Inset: Plot of the measured ratio $^{65}T_1/^{63}T_1$ against temperature for $Y_{0.9}Ca_{0.1}Ba_2Cu_3O_7$ (open circles) and $Y_{0.8}Ca_{0.2}Ba_2Cu_3O_7$ (filled circles).

Further evidence for no significant apparent change in the antiferromagnetic correlation length, within the MMP model and using the BP scaling analysis for overdoped $Y_{1-x}Ca_xBa_2Cu_3O_7$ ($p<0.233$), is provided by $^{63}T_{2g}$. We plot in Fig. 3 the spin-echo decay from $Y_{0.9}Ca_{0.1}Ba_2Cu_3O_7$ (filled circles, $p=0.214$) at 80 K and $YBa_2Cu_3O_7$ [filled-up triangles, $p=0.16$ (Ref. 14)] at 78 K, along with the fit to the data using Eq. (1). Note that the data in Fig. 3 have already been corrected for the Redfield contribution [first factor in Eq. (1)]. The resultant NQR $1/^{63}T_{2g}$ is (6.5 ± 0.3) ms^{-1} for $Y_{0.9}Ca_{0.1}Ba_2Cu_3O_7$. This can be compared to the NQR $1/^{63}T_{2g}$ of (7.9 ± 0.2) ms^{-1} in $YBa_2Cu_3O_7$. Within the MMP model and assuming that $\xi\gg1$, it is possible to express $1/^{63}T_{2g}$ as $1/^{63}T_{2g}\propto\beta\xi$.[6,18] Hence $1/^{63}T_{2g}$ provides a direct measure of ξ. Therefore, from the measurements of $1/^{63}T_{2g}$ in $YBa_2Cu_3O_7$ and $Y_{0.9}Ca_{0.1}Ba_2Cu_3O_7$ we conclude that within the MMP model, ξ decreases by only ~20%. A small decrease in ξ, within the MMP model, is consistent with the negligible affect of p on $1/^{63}T_1T$ mentioned above, at least for $p<0.233$.

The observations above that, within the MMP model, ξ does not change significantly in $Y_{1-x}Ca_xBa_2Cu_3O_7$ (for $p<0.233$) appears to contradict recent reports that imply the absence of antiferromagnetic correlations in the overdoped region (possibly only for $p>\sim 0.19$).[1,2] It is therefore important to see if the dominant relaxation mechanism changes in going from the optimally doped to the overdoped region. The dominant relaxation mechanism can be determined from $^{65}T_1/^{63}T_1$. In the case of magnetic relaxation it can be shown that $^{65}T_1/^{63}T_1=(^{63}\gamma/^{65}\gamma)^2$, where γ is the nuclear gyromagnetic ratio.[32] If quadrupole relaxation dominates, then $^{65}T_1/^{63}T_1=(e^{63}Q/e^{65}Q)^2$, where eQ is the nuclear-quadrupole moment.[32]

We plot in Fig. 4 $^{65}T_1/^{63}T_1$ against hole concentration for $Y_{0.9}Ca_{0.1}Ba_2Cu_3O_7$ at 80 K and $Y_{0.8}Ca_{0.2}Ba_2Cu_3O_7$ at 68 K. For comparison, we include $^{65}T_1/^{63}T_1$ for optimally doped $YBa_2Cu_3O_{7-\delta}$ near 60 K.[32] The relationship between hole concentration and T_c is shown by the dashed curve (right axis). It is clear that $^{65}T_1/^{63}T_1$ does not change on the overdoped side and there is no departure from magnetic scattering. We show in the inset to Fig. 4 that $^{65}T_1/^{63}T_1$ does not show any variation for moderate temperatures above T_c.

Similar measurements of $^{65}T_{2g}/^{63}T_{2g}$ were made on the $Y_{0.9}Ca_{0.1}Ba_2Cu_5O_7$ sample at 80 K. We find that the resultant ratio is $^{65}T_{2g}/^{63}T_{2g}=1.19\pm 0.10$. This can be compared with the theoretical estimate of 1.30 obtained from $^{65}T_{2g}/^{63}T_{2g}=(^{63}\gamma/^{65}\gamma)^2(^{63}P/^{65}P)^{0.5}$, where ^{63}P and ^{65}P are the isotopic abundances of ^{63}Cu and ^{65}Cu, respectively.[33] One study on $YBa_2Cu_4O_8$ ($p=0.122$) found that for NQR, $^{65}T_{2g}/^{63}T_{2g}$ is close to the theoretical estimate where the experimental ratio is 1.25 ± 0.03.[19] It has been shown that the charge and spin dynamics on the CuO_2 planes of $YBa_2Cu_4O_8$ are essentially the same as underdoped $YBa_2Cu_2O_{7-\delta}$ with a δ of ~ 0.2.[34] Consequently, we find that $^{65}T_{2g}/^{63}T_{2g}$ for overdoped $Y_{0.9}Ca_{0.1}Ba_2Cu_3O_7$ is comparable to that in the underdoped cuprates.

In conclusion, we find that from NQR measurements on overdoped $Y_{1-x}Ca_xBa_2Cu_3O_7$ within the MMP model, the antiferromagnetic correlation length does not significantly decrease on the overdoped side, at least for $p<0.233$. This is inconsistent with recent reports claiming the absence of antiferromagnetic correlations for $p>0.19$ in overdoped HTSC. However, our results do not necessarily contradict the results from a neutron-scattering study on another HTSC, $La_{2-x}Sr_xCuO_4$. It was found that the peak width ($\propto\xi^{-1}$) was weakly dependent on p for $p\leqslant 0.18$ while it was ~ 3.6 times larger for $p=0.25$.[3] Unfortunately, there was no reported data in the $0.18<p<0.25$ hole concentration range. Hence, it is possible that in $La_{2-x}Sr_xCuO_4$ ξ decreases only for $p>0.233$. We also find that the relaxation mechanism is still magnetic on the overdoped side, indicating that magnetic relaxation is still dominant in the overdoped region.

We acknowledge helpful discussions with J. L. Tallon and support from the New Zealand Foundation for Research Science and Technology and the Alexander von Humboldt Foundation.

[1] J. L. Tallon, in *Advances in Superconductivity XII*, edited by T. Yamashita and K. Tanabe (Springer-Verlag, Tokyo, 1999).
[2] J. L. Tallon and J. W. Loram, Physica C **349**, 53 (2001).
[3] K. Yamada, C. H. Lee, K. Kurahashi, J. Wada, S. Wakimoto, S. Ueki, H. Kimura, Y. Endoh, S. Hosoya, G. Shirane, R. J. Birgeneau, M. Greven, M. A. Kastner, and Y. J. Kim, Phys. Rev. B **57**, 6165 (1998).
[4] A. J. Millis, H. Monien, and D. Pines, Phys. Rev. B **42**, 167 (1990).
[5] F. Mila and T. M. Rice, Physica C **157**, 561 (1989).
[6] V. Barzykin and D. Pines, Phys. Rev. B **52**, 13 585 (1995).
[7] D. Pines, Z. Phys. B: Condens. Matter **103**, 129 (1997).
[8] P. Monthoux, A. Balatsky, and D. Pines, Phys. Rev. B **46**, 14 803 (1992).
[9] P. Monthoux and D. Pines, Phys. Rev. B **47**, 6069 (1993).
[10] P. Monthoux and D. Pines, Phys. Rev. B **49**, 4261 (1994).
[11] M. Takigawa, J. L. Smith, and W. L. Hults, Phys. Rev. B **44**, 7764 (1991).
[12] M. Takigawa, A. P. Reyes, P. C. Hammel, J. D. Thompson, R. H. Heffner, Z. Fisk, and K. C. Ott, Phys. Rev. B **43**, 247 (1991).
[13] T. Auler, M. Horvatić, J. A. Gillet, C. Berthier, Y. Berthier, P. Ségransan, and J. Y. Henry, Phys. Rev. B **56**, 11 294 (1997).
[14] S. Krämer and M. Mehring, Phys. Rev. Lett. **83**, 396 (1999).
[15] S. Fujiyama, Y. Itoh, H. Yasuoka, and Y. Ueda, J. Phys. Soc. Jpn. **66**, 2864 (1997).
[16] G. V. M. Williams, J. L. Tallon, R. Michalak, and R. Dupree, Phys. Rev. B **57**, 8696 (1998).
[17] G. V. M. Williams, J. L. Tallon, and R. Meinhold, Phys. Rev. B **52**, 7034 (1995).
[18] N. J. Curro, T. Imai, C. P. Slichter, and B. Dabrowski, Phys. Rev. B **56**, 877 (1997).
[19] N. J. Curro and C. P. Slichter, J. Magn. Reson. **130**, 186 (1998).
[20] R. L. Corey, N. J. Curro, K. O'Hara, T. Imai, C. P. Slichter, K. Yoshimura, M. Katah, and K. Kosuge, Phys. Rev. B **53**, 5907 (1996).
[21] M. R. Presland, J. L. Tallon, R. G. Buckley, R. S. Liu, and N. E. Flower, Physica C **176**, 95 (1991).
[22] M. Lee, W. P. Halperin, and K. Poeppelmeier, Physica C **329**, 185 (2000).
[23] A. J. Vega, W. E. Farneth, E. M. McCarron, and R. K. Bordia, Phys. Rev. B **39**, 2322 (1989).
[24] T. Machi, I. Tomeno, T. Miyatake, K. Tai, N. Koshizuka, S. Tanaka, and H. Yasuoka, Physica C **185-189**, 1147 (1991).
[25] S. P. Klein, R. Wang, A. W. Sleight, and W. W. Warren, Jr., Phys. Rev. B **56**, 6335 (1997).
[26] K. Ishida, Y. Kitaoka, N. Ogata, T. Kamino, K. Asayama, J. R. Cooper, and N. Athanassopoulou, J. Phys. Soc. Jpn. **62**, 2803 (1993).
[27] P. C. Hammel, M. Takigawa, R. H. Heffner, Z. Fisk, and K. C. Ott, Phys. Rev. Lett. **63**, 1992 (1989).

[28] G. V. M. Williams, J. L. Tallon, and J. W. Loram, Phys. Rev. B **58**, 15 053 (1998).
[29] K. Magiahi, Y. Kitaoka, G.-q. Zheng, K. Asayama, T. Kondo, Y. Shimakawa, T. Manako, and T. Kubo, Phys. Rev. B **54**, 10 131 (1996).
[30] G. V. M. Williams, *Studies of High Temperature Superconductors* (Nova Science, New York, 1999), Vol. 27, p. 113.
[31] G. V. M. Williams, D. J. Pringle, and J. L. Tallon, Phys. Rev. B **61**, 9257 (2000).
[32] M. Takigawa, J. L. Smith, and W. L. Hults, Phys. Rev. B **44**, 7764 (1991).
[33] C. H. Pennington, D. J. Durand, C. P. Slichter, J. P. Rice, E. D. Bukowski, and D. M. Ginsberg, Phys. Rev. B **39**, 274 (1989).
[34] R. Dupree, Z. P. Han, D. McPaul, T. G. N. Babu, and C. Greaves, Physica C **179**, 311 (1991).